



---

*Research article*

## **Modulation of the mechanical properties of ventricular extracellular matrix hydrogels with a carbodiimide crosslinker and investigation of their cellular compatibility**

**Kyohei Fujita<sup>1</sup>, Zhonggang Feng<sup>1\*</sup>, Daisuke Sato<sup>2</sup>, Tadashi Kosawada<sup>1</sup>, Takao Nakamura<sup>2</sup>, Yasuyuki Shiraishi<sup>3</sup> and Mitsuo Umezu<sup>4</sup>**

<sup>1</sup> Graduate School of Science and Engineering, Yamagata University, Yonezawa, Japan

<sup>2</sup> Graduate School of Medical Science, Yamagata University, Yamagata, Japan

<sup>3</sup> Institute of Development, Aging, and Cancer, Tohoku University, Sendai, Japan

<sup>4</sup> Integrative Bioscience and Biomedical Engineering, Waseda University, Tokyo, Japan

\* **Correspondence:** Email: zhgfeng@yz.yamagata-u.ac.jp.

**Abstract:** Hydrogels made from the cardiac extracellular matrix (ECM) as two-dimensional (2D) or 3D cell-culture substrates have beneficial biochemical effects on the differentiation of stem cells into cardiomyocytes. The mechanical properties of the substrates that match those of the host tissues have been identified as critical biophysical cues for coaxing the tissue-specific differentiation of stem cells. The objectives of the present study are (1) to fabricate hydrogels comprising pure ventricular ECM (vECM), (2) to make the gels possess mechanical properties similar to those of the decellularized ventricular tissue, and (3) to evaluate the cellular compatibility of the hydrogels. In order to achieve these aims, (1) a simplified protocol was developed to produce vECM solution easily and rapidly, (2) N-(3-Dimethylaminopropyl)-N'-ethylcarbodiimide hydrochloride (EDAC) was chosen to crosslink the hydrogels made from the vECM solution to enhance their mechanical properties and stabilize the microstructure of the gels, (3) rat embryonic fibroblasts or cardiomyocytes were cultured on these gels to determine the cellular compatibility of the gels. In particular, the nonlinearity and viscoelasticity of the gels were characterized quantitatively using a newly proposed nonlinear Kelvin model. The results showed that EDAC treatment allowed modulation of the mechanical properties of the gels to the same level as those of decellularized ventricular tissue in terms of the equilibrium

elasticity and relaxation coefficient. Cell culture confirmed the cellular compatibility of the gels. Furthermore, an empirical relationship between the equilibrium elastic modulus of the gels and the vECM and EDAC concentrations was derived, which is important to tailor the mechanical properties of the gels. Finally, the influence of the mechanical properties of the gels on the behavior of cultured fibroblasts and cardiomyocytes was discussed.

**Keywords:** ventricular extracellular matrix; decellularization; hydrogel; nonlinearity; viscoelasticity; cellular biocompatibility

---

## 1. Introduction

Cardiac tissue engineering shows great promise in modeling heart functions, developing modalities to treat heart failure, and screening new pharmaceutical drugs [1]. Cardiomyocytes (CMs) have a limited ability to regenerate themselves; therefore, embryonic stem cells (ESCs) or induced pluripotent stem cells (iPSCs) are regarded as the most promising cell source for generating CMs to construct cardiac tissue [2]. The most frequently used method to differentiate ESCs and iPSCs into CMs is to expose these stem cells to various cardiogenesis-related factors supplemented in culture medium in a temporal series that mimics the process of cardiogenesis *in vivo* [3–5]. However, recent studies suggest that cell culture scaffolds derived from the cardiac extracellular matrix (ECM) have beneficial effects on cardiac differentiation. It was reported that the cardiac differentiation was enhanced by culturing embryoid bodies of human ESCs in hydrogels comprising cardiac ECM and type I collagen, without supplementation of the commonly used differentiation factors in culture medium [6]. Another study reported that mouse ESCs cultured on decellularized myocardial or liver tissues differentiated into cardiomyocytes or hepatocytes, respectively [7]. These studies showed that tissue-specific native ECM has a determinant biochemical impact on the tissue-specific differentiation of stem cells.

On the other hand, mechanical properties of cell culture substrates have been identified as critical biophysical cues for cellular-fate processes including differentiation of stem cells. Altering the elasticity of culture substrates can drive human mesenchymal stem cells toward neurogenic, myogenic, or osteogenic differentiation [8]. More recently, it was reported that stress relaxation of hydrogels has a significant influence on cellular behavior, as well as the differentiation of stem cells [9].

In light of the abovementioned discoveries, we aimed to develop a cell culture substrate made from pure ventricular ECM (vECM) in hydrogel form, which possesses similar mechanical properties to decellularized ventricular tissue. In our future study, we are going to utilize this substrate for promoting the cardiac differentiation of stem cells, both biochemically and biophysically.

The choice of the hydrogel form as the culture substrate is because of its ease of formation into specific geometries and its potential for angiogenesis in the construction of 3-dimensional tissue [10]. However, hydrogels made from vECM are too fragile to achieve the same mechanical properties as

native cardiac tissue. Another problem is that the microstructure of hydrogels is unstable, which might result in the microscale or macroscale collapse of the structure when used as a cell culture substrate because of the tense cell-substrate interactions [11,12].

There are three major ways to improve the mechanical properties of ECM hydrogels: increasing the ECM concentration [13,14]; blending the ECM with other natural or synthetic polymers (e. g., collagen I [6], fibrin [15], and polyethylene glycol [16]); and using chemical crosslinkers [17,18]. The first method can only produce a limited improvement in the mechanical properties of the gels and it cannot solve the problem of structural instability. The second method contradicts our aim of making hydrogels from pure vECM; the blended composites might disrupt the activities of the beneficial factors within the vECM. Consequently, we chose *N*-(3-Dimethylaminopropyl)-*N'*-ethylcarbodiimide hydrochloride (EDAC) as a crosslinker to improve the mechanical properties of the gels and to stabilize the microstructure. The study took advantage of the unique crosslinking mechanism of EDAC. EDAC modifies the side chains of amino acid residues in proteins to make them react with other side chains, and to mediate ester bond formation between the hydroxyl and carboxyl groups, resulting in the so-called zero-length crosslinking [18]. The by-product of the crosslinking, which is water-soluble urea, can be rinsed away easily, such that there are no additional substances incorporated into the matrix. This mechanism favored our aim of creating pure and stable vECM gels for the cardiac differentiation of stem cells.

In this paper, we report the method to fabricate vECM hydrogels, the assessment of the mechanical properties of the gels modulated by EDAC treatment, and the cell-culture compatibility of the EDAC-treated vECM gels in terms of fibroblast attachment and proliferation, the cytotoxicity assay for the fibroblasts, and the beat rate of cardiomyocytes cultured on the gels. In particular, the nonlinear viscoelasticity of the gels was investigated thoroughly using uniaxial compression and a newly proposed nonlinear Kelvin-type theoretical model [19,20]. The influence of the mechanical properties of the gels on the behavior of the cultured fibroblasts and cardiomyocytes was also discussed.

## 2. Materials and methods

### 2.1. vECM gel formation and the crosslink treatment

Heart ventricles of adult Japanese Saanen goats were sliced (ca. 2 mm), cut into small pieces, soaked in 1 N saline solution (Sigma-Aldrich, St. Louis, MO, USA) for 2 h, and rinsed with deionized water (DW) twice, each for 15 min. The pieces were decellularized by stirring in the solution of 1% (w/v) sodium dodecyl sulfate (Sigma-Aldrich) in phosphate buffered saline (PBS) for 4–5 days, following in a solution of 1% (w/v) Triton X-100 (Wako, Japan) in PBS for 24 hours. This process could be repeated once more depending on the state of decellularization. After decellularization, the pieces of vECM were rinsed with DW for 3 days, further homogenized, and then immediately digested with pepsin (Sigma-Aldrich,  $\geq 2500$  units/mg) in 10 mM HCl (Wako) solution for 48 h to produce vECM solutions at concentrations of 15–22 mg/mL. The mass ratio of pepsin to tissue was 1:250. Finally, the vECM solutions were adjusted to pH 7.4 and to a salt concentration equivalent to  $1\times$  PBS using 1.0 M NaOH and  $10\times$  PBS, respectively. To quantify the

weight of the vECM in the solution, 500  $\mu\text{L}$  of vECM solution on a petri-dish was dried at 70  $^{\circ}\text{C}$  overnight and the weight of the dried vECM was measured with an analytical balance to determine the vECM concentration. Before this study, the procedure to produce the ECM solution involved lyophilization and milling of decellularized ECM before digestion [6,13–16]. Our protocol omitted these steps so that the vECM solutions were produced swiftly and with much lower equipment investment.

For the formation of vECM gels, the vECM solutions were first diluted to 7.5 mg/mL, 12.5 mg/mL, and 17.5 mg/mL with  $1\times$  PBS. For each gel, 400  $\mu\text{L}$  of vECM solution at one of the above concentrations was poured into a circular casting mold, which is a well with diameter of 12.5 mm made by cutting a 5 mm-thick silicone plate. The gel formed after 1 h at 37  $^{\circ}\text{C}$ . The above processes were performed under sterile conditions. Images of the decellularized tissue, a vECM solution, and a vECM gel are shown in Figure 1.

For the crosslinking treatment of the gels by EDAC (Sigma-Aldrich), vECM gels were immersed in EDAC-DW solutions at concentrations of 10 mM, 30 mM, 50 mM, or 100 mM for 24 h at room temperature. After the treatment, the gels were rinsed in DW for 2 days. In this paper, the types of vECM gels are denoted as  $xx$  mM EDAC- $yy$  mg/mL gel, which indicates that the gel consisted of vECM at  $yy$  mg/mL that was treated with EDAC solution at  $xx$  mM.

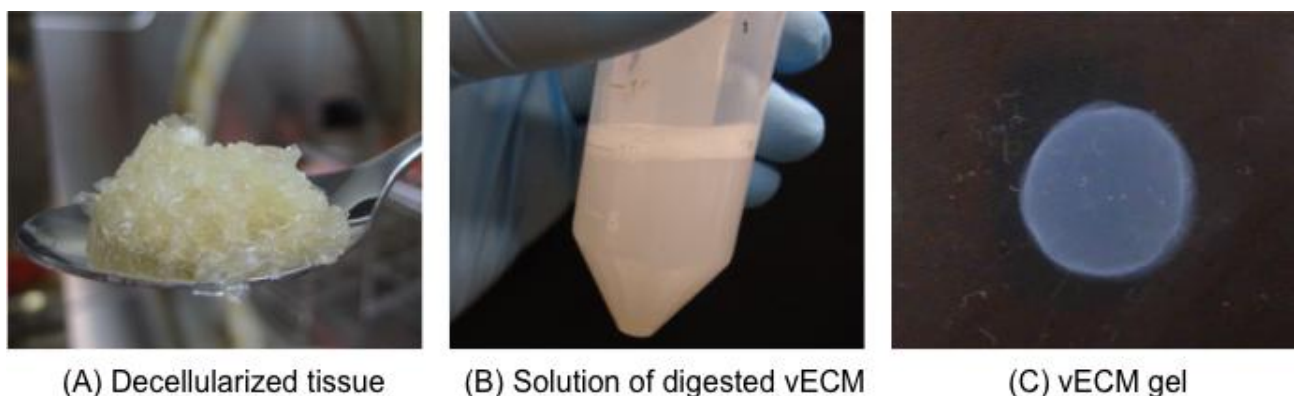


**Figure 1.** Decellularization of the goat ventricle tissue and the processes of gelation. (a) Tissue decellularized by SDS + Triton X-100 method, (b) vECM solution produced using pepsin digestion, (c) a vECM hydrogel.

## 2.2. Assessment of residual DNA content in vECM solutions

DNA in vECM solutions was extracted by using ISOGEN (NIPPON GENE, Japan) and precipitated from the intermediate phase and organic phase by ethanol method. The extracted DNA was washed with ethanol, dried at room temperature, and resuspended in Tris-EDTA buffer. Quantification of the extracted DNA was conducted with BioSpec-Nano (Shimadzu, Japan). The residual DNA concentration in vECM solution was converted into the DNA content with respect to wet decellularized tissue.

### 2.3. Protein composition of vECM solutions

Mass spectrometry of vECM eluted from sodium dodecyl sulfate-polyacrylamide gel electrophoresis (SDS-PAGE) gels was conducted in order to investigate the protein composition of the vECM. vECM solution (9.0 mg/mL) was loaded in 7.5% acrylamide gel for electrophoresis. Each band in SDS-PAGE gel was cut off for the analysis of protein composition, respectively. The vECM proteins were eluted and further digested by trypsin. Liquid chromatography mass spectrometry (LC-MS) [21] was conducted at RIKEN Kobe Proteomics Facility. The protein composition was estimated by emPAI method [22]. Two vECM samples from different ventricles were analyzed and the average of the composition ratio was presented.

### 2.4. Histological observation

Gel samples were fixed overnight at 4 °C in 4% paraformaldehyde in PBS and embedded in paraffin wax. Samples in the shape of disc were sectioned at longitudinal direction and the sections were deparaffinized. The sections were stained with Picrosirius red staining solution containing 1% Sirius red (Polysciences, PA, USA) and 3% saturated picric acid (Wako, Japan) for 30 min and the stained sections were washed and dehydrated with 100% ethanol. The sections were treated with xylene and mounted. Photos of stained sections were taken by a microscope (OLYMPUS IX71, Olympus, Japan) and binarized through ImageJ. Stained collagen fibrils were transformed into black in the image and the area occupied by them was automatically counted by ImageJ. The ratio of the area of collagen to the whole area was used to assess the degree of formation of collagen fibrillar network. Two samples from each group were investigated.

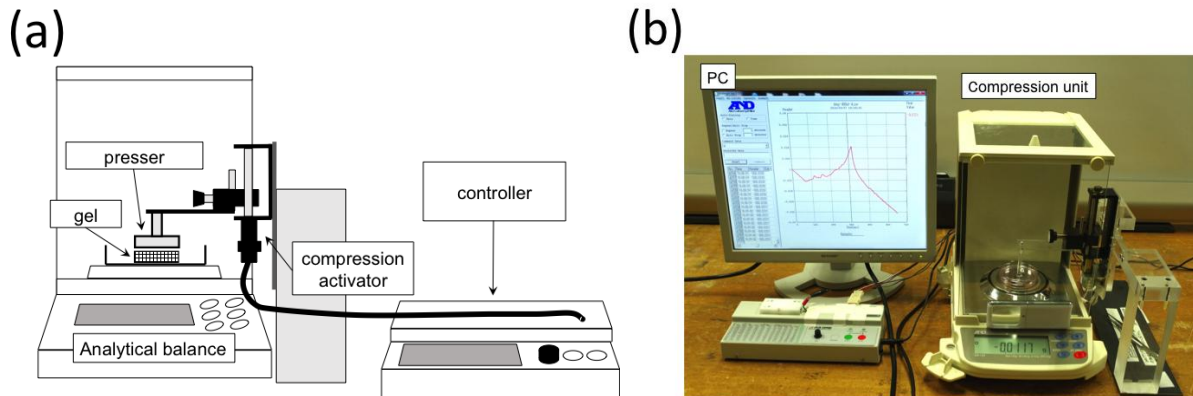
### 2.5. Compression test

Figure 2a shows a schematic representation of the laboratory-made compression-testing machine [19], as seen in Supplementary material, and Figure 2b shows the image of the entire system. A specimen immersed in PBS in a culture dish was placed on the measuring pan of an analytical balance (GR-120, A & D Company, Japan). It was compressed using a presser, which was driven downwards at a constant speed by a step motor. The strain rate was  $0.0007 \pm 0.0001 \text{ s}^{-1}$ . When the compression strain reached 5%, the presser was stopped, and stress relaxation then occurred in the gel. The duration of the relaxation was 5 min. The force exerted during the compression and the relaxation phases was measured by the analytical balance, and the values were input into a computer. The compression stress was calculated by dividing the force by the gel area.

The purpose of the vECM gels is for culture heart cells, which beat at one to several Hz. Relaxation measured over 5 minutes was enough for cardiomyocyte dynamics. For a longer cell culture period, we have done preliminary compression test on the EDAC-treated vECM gels that were immersed in the culture medium for 2 days. As a result, we have not confirmed any significant difference on the mechanical properties of those gels after this period comparable to our culture duration (data was not shown in this paper).

In addition, samples of decellularized ventricular tissue (DV tissue), which were cut out from

decellularized tissue slices with thickness of  $2.1 \pm 0.2$  mm using a  $\phi 12.5$  cork borer (NONAKA RIKAKI, Japan), were also tested in the compression-relaxation experiment.



**Figure 2.** Experimental apparatus for the uniaxial compression test. (a) Schematic representation of the compression-testing unit. (b) Image of the entire system. Details are in Supplementary material.

## 2.6. Mechanical model and data analysis

The Kelvin, Maxwell, and Voigt models are linear models used to characterize the viscoelasticity of materials [23,24]. In this study, we employed a newly proposed nonlinear Kelvin-type model [19,20] to analyze the nonlinear viscoelasticity in the gels. Figure 3 is the diagrammatic representation of the model, which consists of two parallel power-law nonlinear elastic springs and one viscous dashpot in series with one of the springs. The constitutive equation of the nonlinear Kelvin-type model is as follows:

$$\sigma(t) = K_1 \varepsilon^\alpha(t) + K_2 \int_0^t e^{-\frac{t-t'}{\lambda}} d(\varepsilon^\alpha(t')) \quad (1)$$

where  $\sigma$  is the compression stress;  $\varepsilon$  is the compression strain;  $K_1$ ,  $K_2$  are two elastic coefficients; power  $\alpha$  ( $\alpha > 1$ ) indicates the nonlinearity in the relationship between stress and strain (the larger the value of  $\alpha$ , the stronger the nonlinearity); and  $\lambda$  is the stress-relaxation coefficient. The following expressions, corresponding to the compression phase and the relaxation phase in the experiment, can be derived from Eq 1.

$$\sigma(t) = K_1 (ct)^\alpha(t) + \alpha K_2 \int_0^t e^{-\frac{t-t'}{\lambda}} (ct')^{\alpha-1} c dt' \quad (0 \leq t < t_s, \text{ compression phase}) \quad (2)$$

$$\sigma(t) = K_1 (ct_s)^\alpha(t) + K_2 \alpha e^{-\frac{t}{\lambda}} \int_0^{t_s} e^{\frac{t'}{\lambda}} (ct')^{\alpha-1} c dt' \quad (t \geq t_s, \text{ relaxation phase}) \quad (3)$$

where  $t_s$  is the time at the end of the compression phase, and  $c$  is the strain rate. The experimental data in this study were regressed against Eqs 2 and 3 to obtain  $K_1$ ,  $K_2$ ,  $\alpha$ , and  $\lambda$ .

Nonlinearity results in that the coefficients  $K_1$  and  $K_2$  alone are not able to reflect the practical stiffness of the gels without considering the effects of  $\alpha$ . To investigate the practical stiffness and to exclude the viscous effects, we defined the equilibrium elastic modulus  $E$  as follows:

$$E = \frac{K_1 \varepsilon_{max}^\alpha}{\varepsilon_{max}} \quad (4)$$

where  $\varepsilon_{max}$  is the maximum strain;  $\varepsilon_{max}$  was 0.05 in this study.

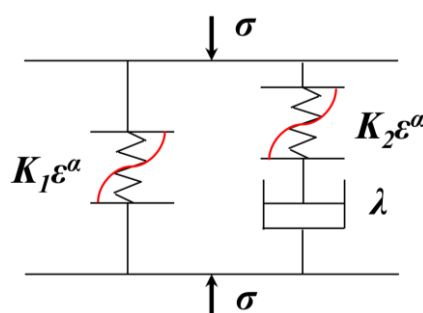


**Figure 3.** Diagrammatic representation of the nonlinear Kelvin model. The model splits external compressional work into two fractions: the first is reversible energy storage in a power-law spring, with coefficient  $K_1$ , and the second is a power-law spring with coefficient  $K_2$ , in which energy is dissipated by an exponential process with relaxation coefficients  $\lambda$ . Power  $\alpha$  ( $\alpha > 1$ ) indicates the nonlinearity.  $\sigma$  is the compression stress.

### 2.7. *In vitro* cell culture

All the animal experimental procedures described in this section were approved by the Animal Research Committee of Yamagata University.

Rat embryonic fibroblasts (REFs) and rat embryonic cardiomyocytes (RECs) were harvested from Wistar rat embryos at 14–18 days after fertilization, following a previously described protocol [25]. Briefly, dermal REFs were harvested by the explant method. Pieces of minced embryonic skin were cultured in Dulbecco's modified Eagle's medium (DMEM; Sigma-Aldrich) supplemented with 10% fetal bovine serum (FBS) and 1% penicillin-streptomycin (Sigma-Aldrich). The outgrown fibroblasts were harvested and passaged 3–5 times for use. To harvest the RECs, the embryonic heart ventricles were cut into pieces, and digested in 0.1% collagenase IV (Sigma-Aldrich) supplemented with 0.1% D-glucose (Sigma-Aldrich) at 37 °C. The primary RECs were cultured in the DMEM/F12-Ham (Sigma-Aldrich) with 10% FBS, 1% penicillin-streptomycin, and 10  $\mu\text{g}/\text{mL}$  human insulin (Eli Lilly, Indianapolis, IN, USA) for use.

The EDAC-treated vECM gels were incubated with the culture medium for 24 h before cell seeding. REFs (5000 cells) and RECs ( $1 \times 10^6$  cells) were seeded on separate vECM gels, and cultured for 4 days. For REF culture, four types of gels (10 mM EDAC-7.5 mg/mL, non-treated 17.5 mg/mL, 30 mM EDAC-12.5 mg/mL, and 10 mM-17.5 mg/mL) were used in each experiment. The cells were stained with Calcein AM (Dojindo, Japan) on each day, and were observed under a microscope (OLYMPUS IX71, Olympus, Japan). The cell attachment area on the first day and cell

numbers on each of the four days were measured from the image of the stained cells using ImageJ. The relative cell number of the REFs was defined as the ratio of the cell number on each day to the cell number on the first day. The beat rate of the RECs was measured by observing the beating RECs on the vECM gels under the microscope.

## 2.8. Cytotoxicity assay

Cell toxicity was evaluated by lactate dehydrogenase (LDH) leakage assay (Cytotoxicity LDH Assay kit, DOJINDO Inc., Japan) with the protocol recommended by the maker. Briefly, fibroblasts were cultured on different gels for 3 days. The absorbance of medium supernatant at 490 nm was measured by a microplate reader (value B); the absorbance of supernatant of cell lysis in the culture medium under the same culture condition was also measured (value A). Then the LDH leakage rate (R) was calculated by  $R = B/(A - B)$ . Cytotoxicity of EDAC treatment was assessed by comparing the LDH leakage rate for EDAC treated gels ( $R_{\text{EDAC}}$ ) with that for non-treated ones ( $R_{\text{non}}$ ). If  $R_{\text{EDAC}} < R_{\text{non}}$ , then it was judged that EDAC treatment was not cytotoxic. Nine types of EDAC-treated gels (10, 50, 100 mM EDAC-treated gels at the three vECM concentrations), two samples for each type, were tested. Average of the LDH leakage rate versus EDAC concentration was presented to evaluate the cytotoxicity of EDAC crosslinking.

## 2.9. Statistical analysis

All data are expressed as mean  $\pm$  the standard deviation (SD). Statistical analysis was performed using JStat software. Significance was determined using one-way analysis of variance (one-way ANOVA) with Tukey's post hoc test. A value of  $p < 0.05$  was considered significant for each test.

## 2.10. The coefficient of determination

The evaluation of the experiment–model agreement was performed by calculating the coefficient of determination,  $R^2$ . In this study,  $R^2$  was defined as  $R^2 = 1 - \sum_{n=1}^N (x_n - x'_n)^2 / \sum_{n=1}^N x_n^2$ , where  $x_n$  is the experimental data and  $x'_n$  denotes the theoretical values of regression.

# 3. Results

## 3.1. Residual DNA content and protein composition of vECM

Residual DNA content was  $8.0 \pm 2.1$  (n = 6) ng per mg of wet decellularized tissue weight. This data is less than that ( $16.6 \pm 3.23$  ng/mg) reported in the research using decellularized heart to engineer a bioartificial heart [26]. Therefore, the degree of decellularization of the vECM was satisfactory for *in vitro* study. Figure 4 shows the SDS-PAGE photograph and the protein composition in vECM identified by LC-MS. It can be seen that the main contents in vECM are collagen type I, III, IV, and V; and 14 types of collagen were detected. It also shows the existence of



other ECM components: fibrillin, laminin, and fibronectin. A glycoprotein, tenascin-X, was also detected in the vECM.

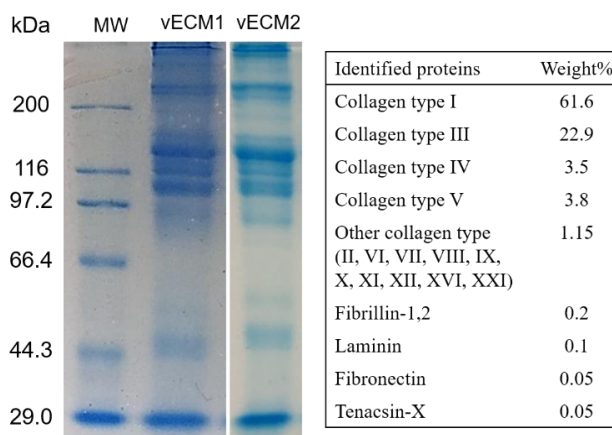


**Figure 4.** SDS-PAGE showing molecular weight bands with standard ladder (on the left). Two samples of vECM solution of different batches were run in this study (vECM1 and vECM2). The inset table showing the protein composition identified by LC-MS.

### 3.2. Histological observation of vECM gels

Figure 5 shows the histological photographs of vECM gels stained with Picrosirium red. It can be seen that the network of collagen fibrils constitutes the skeleton of the vECM gels. Fibril area ratio at the outer portion of the gels was larger than that at the inner portion. Obviously, the collagen fibril area ratio increased with the increase of vECM concentration (by comparison of Figure 5a with Figure 5b). The area ratio tended to increase with the increase of EDAC concentration (by comparison of Figure 5b with Figure 5c), which suggested that EDAC may enhance the formation of collagen fibrils besides crosslinking the fibrils.

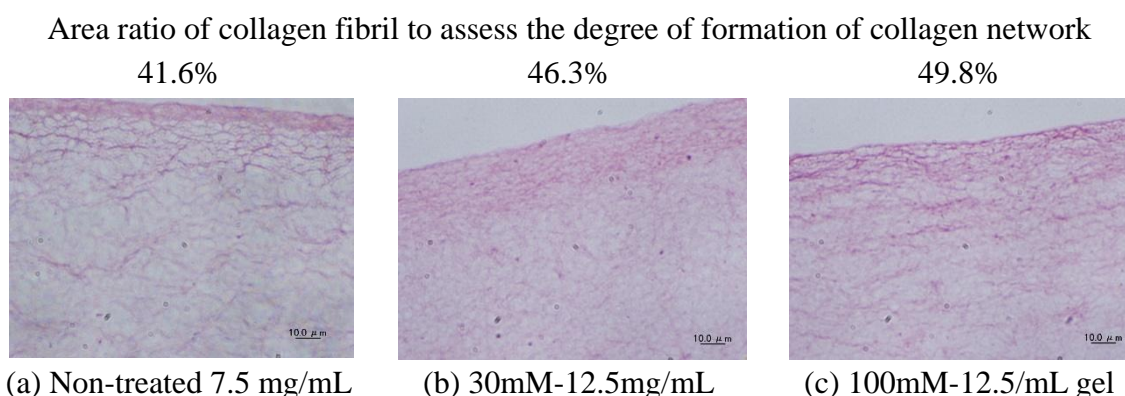


**Figure 5.** Histological photographs of different vECM gels stained with Picrosirium red. Collagen fibrils stained in red and the fibril inhomogeneity in the gels can be observed. Collagen fibril area ratio is shown at the top of each photograph. Scale bars in the pictures represent 10.0 μm.

### 3.3. Viscoelasticity and nonlinearity of vECM gels

Four samples of each type of vECM gels and DV tissue were tested in compression experiment. Figures 6a–6c present the experimental data of a single sample for each type of vECM gels and their regressions via the nonlinear Kelvin model. Stress relaxation and nonlinearity were observed in all samples, and the nonlinear Kelvin model could regress the experimental data with good agreement. A nonlinear toe region in the compression phase appeared in all samples and those for the 10, 30, 50, and 100 mM EDAC-12.5 mg/mL gels and 17.5 mg/mL gels were quite obvious. The nonlinearity increased with increasing vECM and EDAC concentrations (also indicated by the large  $\alpha$  values of these gels in Figure 7d). Figure 6d shows data of decellularized ventricular tissue (DV tissue) and its regression via the nonlinear Kelvin model. The power  $\alpha$  of DV tissue was  $1.3 \pm 0.1$ , which was smaller than that of all the gel samples (Figure 7d), indicating that the nonlinearity of vECM gels was higher than that of the DV tissue.

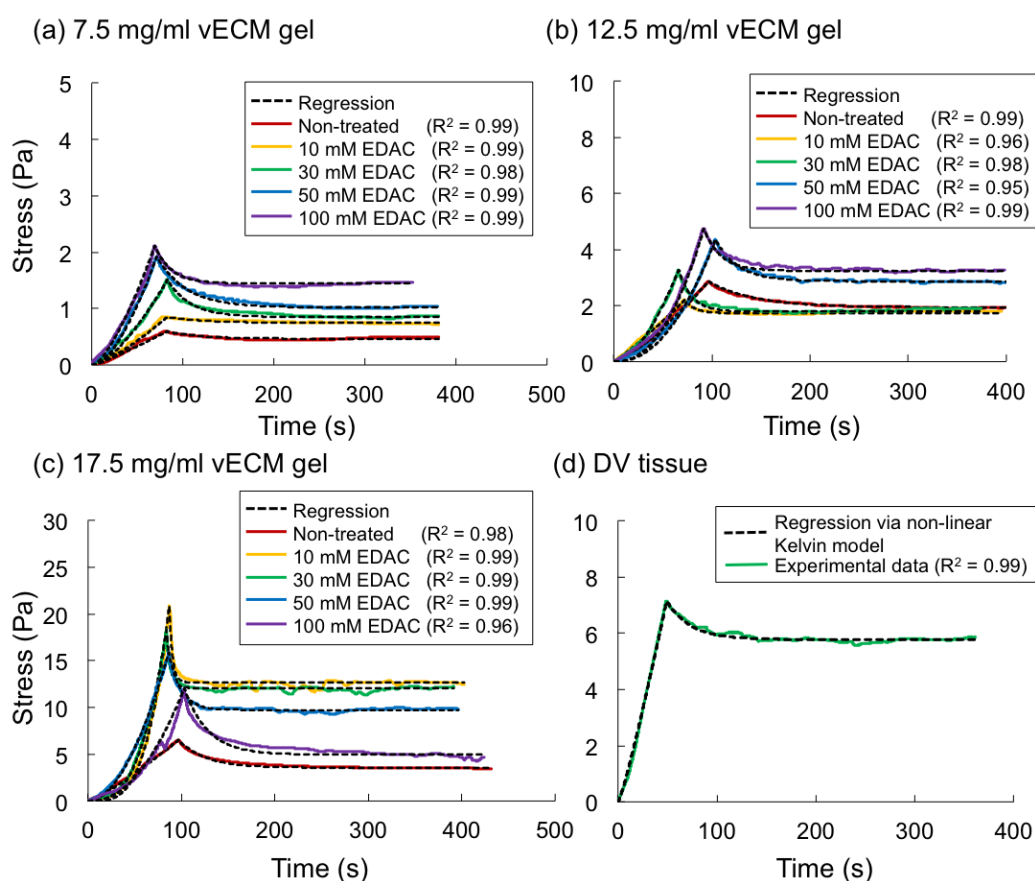


**Figure 6.** Experimental data of compression test on each type of the non-treated and EDAC-treated vECM gels and their regressions obtained through the nonlinear Kelvin model; (a) 7.5 mg/mL vECM gel, (b) 12.5 mg/mL vECM gel, (c) 17.5 mg/mL vECM gel, (d) DV tissue. Four samples were tested for each type of gels and DV tissue ( $n = 4$ ). The figures only show data of a single sample for each type. These figures show the nonlinearity and stress relaxation in the samples and the good agreement between experimental data and the nonlinear Kelvin model.

### 3.4. Modulation of mechanical properties by EDAC treatment

Figures 7a–7d present the mean  $\pm$  SD of  $K_1$ ,  $K_2$ ,  $\lambda$ , and  $\alpha$  of the vECM gels individually. The shadowed bands in these figures show the ranges of the respective parameters of the DV tissue. The elastic coefficients  $K_1$  and  $K_2$  increased with increasing vECM concentration but stress relaxation  $\lambda$  decreased with increasing the vECM concentration (Figures 7a–7c). Meanwhile, the relaxation coefficients of the non-treated vECM gels were close to that of the DV tissue.

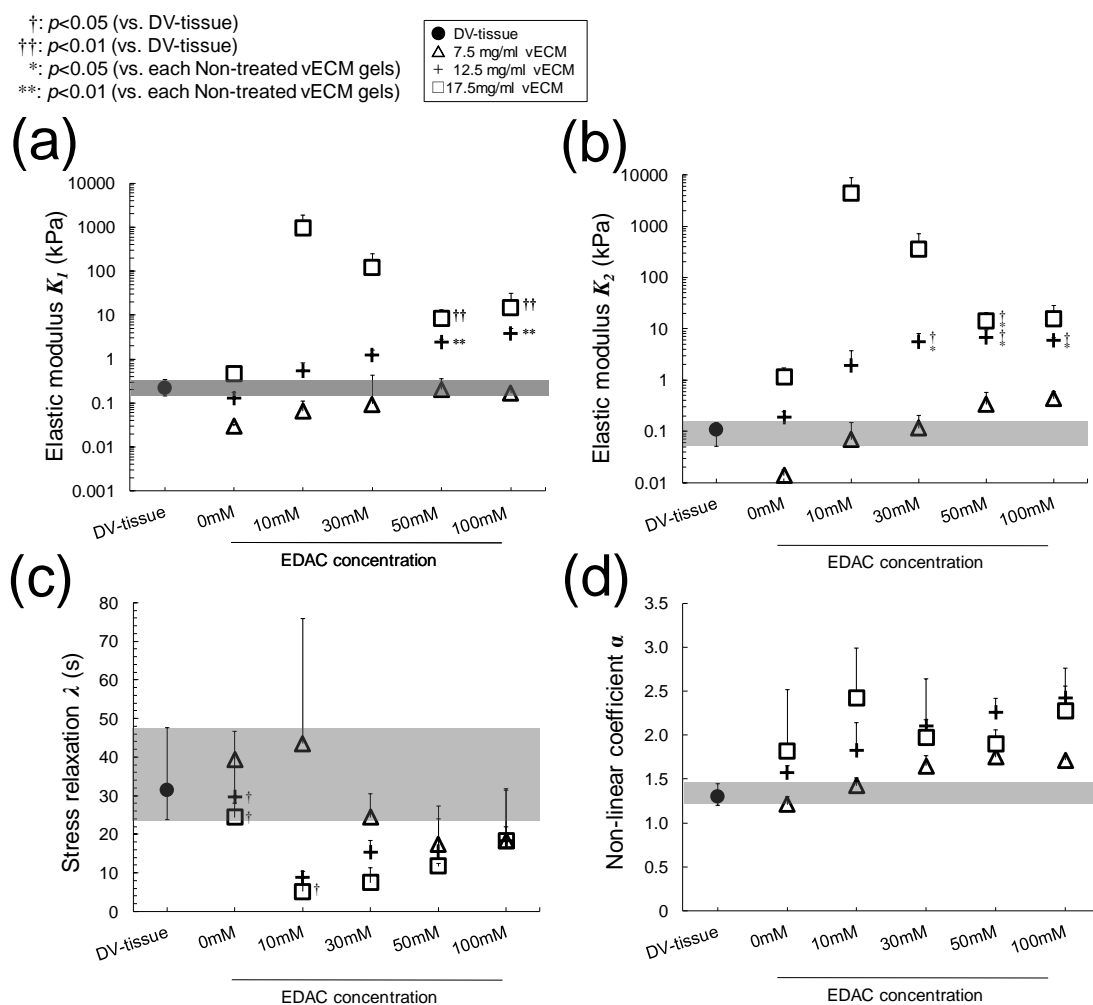


**Figure 7.** Parameters of the nonlinear Kelvin model for vECM and DV tissue. (a)  $K_1$ , (b)  $K_2$ , (c)  $\lambda$ , and (d)  $\alpha$  (Mean  $\pm$  SD.  $n = 4$ ). The thin black band in the figures denotes the range between the maximum value and the minimum value of each parameter for the DV tissue. EDAC treatment can remarkably modulate these parameters.

The effects of EDAC treatment on the mechanical behavior of vECM gels were complicated. The elastic coefficients  $K_1$  and  $K_2$  increased with increasing EDAC concentration in gels at small vECM concentrations (7.5 and 12.5 mg/mL, Figures 7a and 7b). However, there existed “irregular points” at 10 mM and 30 mM EDAC concentrations for the gels at large vECM concentration (17.5 mg/mL); at these points the elastic coefficients were much larger than those at higher EDAC

concentrations (50 and 100 mM, Figures 7a and 7b). Mooney's group studied the mechanical behavior of alginate hydrogels cross-linked with polyethylene glycol diamines and found that the elastic moduli achieved the maximum at certain crosslinker concentration [27,28], a phenomenon similar to the "irregular points" revealed in this study. They postulated that it was due to the formation of second network of macromolecule. As for our material, the formation of second network of other components in the vECM (referring Figure 4) at its large concentration is sufficiently considerable. However, the exact mechanism for this irregular phenomenon needs to be further investigated. For the effect on stress relaxation (Figure 7c), EDAC treatment reduced the stress relaxation coefficient  $\lambda$  in gels at vECM concentrations of 12.5 and 17.5 mg/mL; and the reduction became weak with increasing the EDAC concentration. Whereas, the relaxation coefficient  $\lambda$  of 7.5 mg/mL gels was greatest at 10 mM-EDAC treatment. These "irregular points" may reflect the structural complexity of the vECM gels due to the interaction of the EDAC with other vECM compositions. Figure 7d shows that the higher the concentration of vECM or the higher the concentration of EDAC, the stronger the nonlinearity of the gels; and as mentioned above, the nonlinearity of the DV tissue was the lowest.

The presence of nonlinearity means that the coefficients  $K_1$  and  $K_2$  alone are not able to reflect the practical stiffness of the gels without considering the effects of  $\alpha$ . To investigate the practical stiffness of the gels, we computed the equilibrium elastic modulus  $E$  of the gels as defined by Eq 4. Figure 8a shows that the equilibrium elastic modulus  $E$  increased with increasing vECM concentration. For the effect of EDAC treatment on  $E$ , we found that the following empirical formula could express the relationship between  $E$  and EDAC concentration:

$$E = E_0 e^{\gamma C_{EDAC}} \quad (5)$$

where  $E_0$  is the  $E$  of non-treated vECM gels;  $C_{EDAC}$  is the EDAC concentration;  $\gamma$  is a coefficient. This relationship appears as straight lines on the single logarithmic plot (straight lines in Figure 8a). The highest modulus achieved with a 30 mM crosslinking concentration for 17.5 mg/mL gels was consistent with the "irregular point" phenomenon also presenting in Figures 7a and 7b, which was postulated due to the formation of second network of macromolecule by referring [27,28]. We found that the values of the coefficient  $\gamma$  were almost constant for different vECM concentrations ( $\gamma = 0.0064$  for 7.5 mg/mL vECM gels,  $\gamma = 0.0066$  for 12.5 mg/mL vECM gels, and  $\gamma = 0.0069$  for 17.5 mg/mL vECM gels). Therefore, we used its average value, 0.0066.

Furthermore,  $E_0$  had an almost perfect linear relationship with vECM concentration on a logarithmic plot (Figure 8b), which implied that  $E_0$  could be expressed as follows:

$$E_0 = 2.3e^{0.23C_{ECM}} \quad (6)$$

Ultimately, we obtained an empirical formula for equilibrium elastic modulus under the gel conditions used in this study:

$$E = 2.3e^{0.23C_{ECM} + 0.0066C_{EDAC}} \quad (7)$$

where the units of  $E$ ,  $C_{ECM}$ , and  $C_{EDAC}$  are Pa, mg/mL, and mM, respectively.

Linearity between  $E$  and  $C_{EDAC}$  on the single logarithm plot held well at small vECM concentrations ( $r^2 = 0.82$  for 7.5 mg/mL gels and  $r^2 = 0.69$  for 12.5 mg/mL gels) but deteriorated at

large vECM concentration ( $r^2 = 0.37$  for 17.5 mg/mL gels) due to the existence of “irregular points” at 10 and 30 mM vECM concentrations. However, since  $\gamma$  for all gels at different vECM concentrations were almost constant and the relationship between  $\ln(E_0)$  and vECM concentration was nearly perfect linear (Figure 8b), It suggests that Eq 5 captures the elastic characteristics of collagen fibril skeleton in the vECM gels under different vECM and EDAC concentrations.

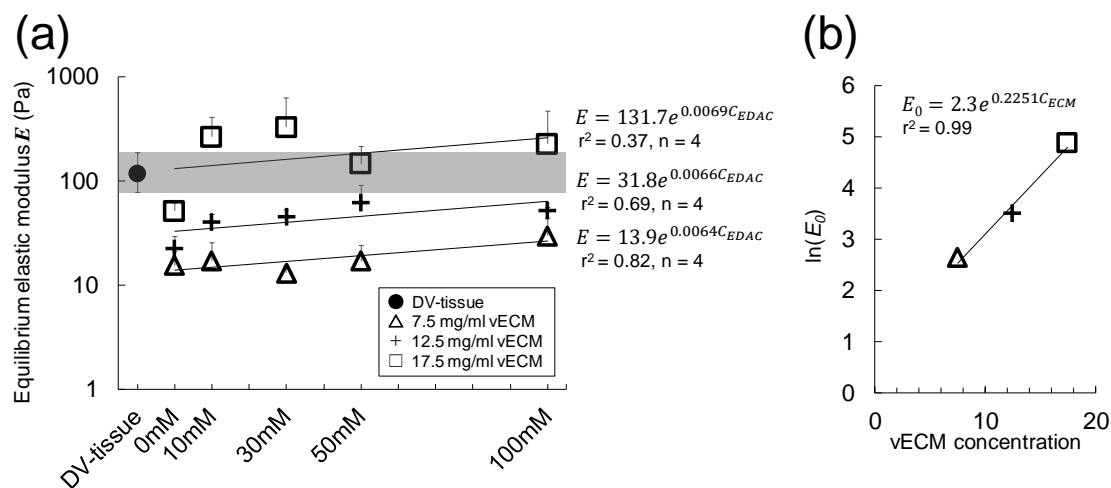


**Figure 8.** (a) Equilibrium elastic modulus,  $E$ , of each vECM gel ( $n = 4$ ). The empirical Eq 5 for each vECM gel of equal concentration is denoted by the straight lines on this logarithmic plot ( $r^2$  is the linear correlation). (b) Relationship between  $E_0$  ( $E$  of non-treated vECM gels) and vECM concentration. Formulas on the plot (a) are the least square regressions of Eq 5 to gels with the same vECM concentration. Formula on plot (b) is Eq 6, a least square regression on the relationship between the equilibrium elasticity of the non-treated gels and the concentration of vECM.

### 3.5. Cell culture compatibility

Finally, we investigated the behavior of cells cultured on the vECM gels treated with EDAC. Table 1 lists the gels that were used as cell-culture substrates in this study, along with their mechanical properties and those of the DV tissue. We chose the following four types of vECM gels as substrates for the REF culture: 10 mM EDAC-7.5 mg/mL gel, which has an equilibrium elastic modulus that is much lower than that of the DV tissue, but possesses almost the same stress relaxation coefficient; non-treated 17.5 mg/mL gel, which has an equilibrium elastic modulus slightly lower than that of the DV tissue, and possesses almost the same stress relaxation coefficient; 30 mM EDAC-12.5 mg/mL gel which has an equilibrium elastic modulus slightly lower than that of the DV tissue, and exhibits a relatively faster stress relaxation; and 10 mM EDAC-17.5 mg/mL gel which has an equilibrium elastic modulus much higher than that of the DV tissue, and exhibits much faster stress relaxation.

Figure 9 shows the images of the cells stained with Calcein AM on the first day. REFs were able to adhere to all the vECM gels with cell protrusions. Figure 10a shows the relative cell number of the

REFs during culture. Figure 10b shows the relative cell number on the fourth day. The cell relative cell number on the vECM gels treated with EDAC was significantly higher than that on the non-treated 17.5 mg/mL gel (Figure 10b), but was the same as that in the culture dish during the first 3 days, showing that EDAC treatment did not impair the cellular compatibility of the gels. The proliferation in the culture dish was much higher than on the vECM gels on the fourth day, which was consistent with the fact that fibroblasts proliferate much faster on hard plastic surfaces in the growth phase than on a soft substrate [29]. Figure 10c shows the difference in the area of attachment of individual REFs on different vECM gels. The average area of individual cells on the vECM gels had an inverse relationship with the relative cell number, i.e., a smaller attachment area corresponded to a higher proliferation. Figure 10d shows that the LDH leakage rate of EDAC-treated gels was smaller than that of non-treated gels, which means that EDAC treatment is not harmful and may enhance the cellular compatibility.

**Table 1.** List of the vECM gels that were used as substrates for cell culture in this study. Each “√” symbol in the table shows that the respective evaluation was conducted.

	$E$ (Pa)	$\lambda$ (s)	Cellular evaluations		
			Cell area of REFs	Proliferation of REFs	Beat rates of RECs
10 mM EDAC-7.5 mg/mL gel	17.1 ± 8.5	43.4 ± 32.5	√	√	√
Non-treated 17.5 mg/mL gel	51.5 ± 9.5	24.3 ± 3.8	√	√	
30 mM EDAC-12.5 mg/mL gel	45.7 ± 6.5	15.2 ± 3.2	√	√	
50 mM EDAC-12.5 mg/mL gel	61.8 ± 29.7	15.5 ± 8.4			√
10 mM EDAC-17.5 mg/mL gel	246.6 ± 147.2	5.1 ± 3.3	√	√	
DV tissue	107.9 ± 42.2	31.4 ± 9.5			

EDAC, *N*-(3-Dimethylaminopropyl)-*N'*-ethylcarbodiimide hydrochloride; vECM, ventricular extracellular matrix; DV tissue, decellularized ventricular tissue; REFs, rat embryonic fibroblasts; RECs, rat embryonic cardiomyocytes;  $E$  (Pa), equilibrium elastic modulus;  $\lambda$  (s), stress relaxation coefficient.

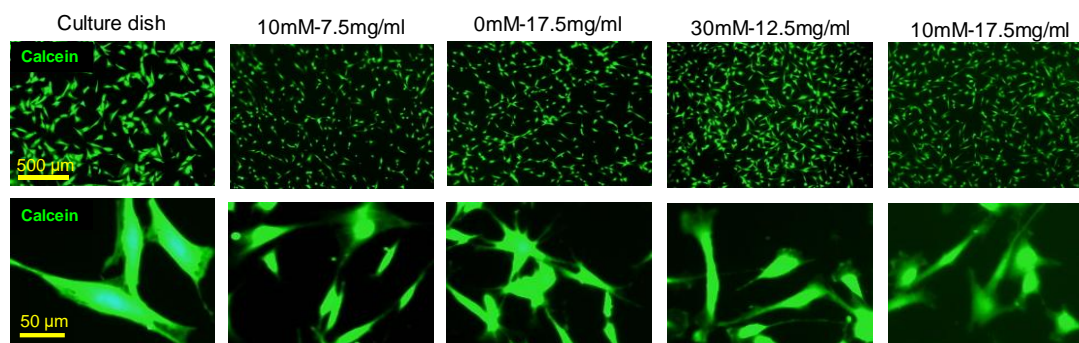


**Figure 9.** Rat embryonic fibroblasts (REFs) seeded after 24 h, and stained with Calcein AM. The panels in the upper row were taken at  $\times 40$  magnitude of microscope and those in the lower row were their zoom in at  $\times 100$  magnitude. REFs were able to adhere to all the vECM gels with cell protrusions. Scale bar =  $500 \mu\text{m}$  in the upper row and  $50 \mu\text{m}$  in the lower row.

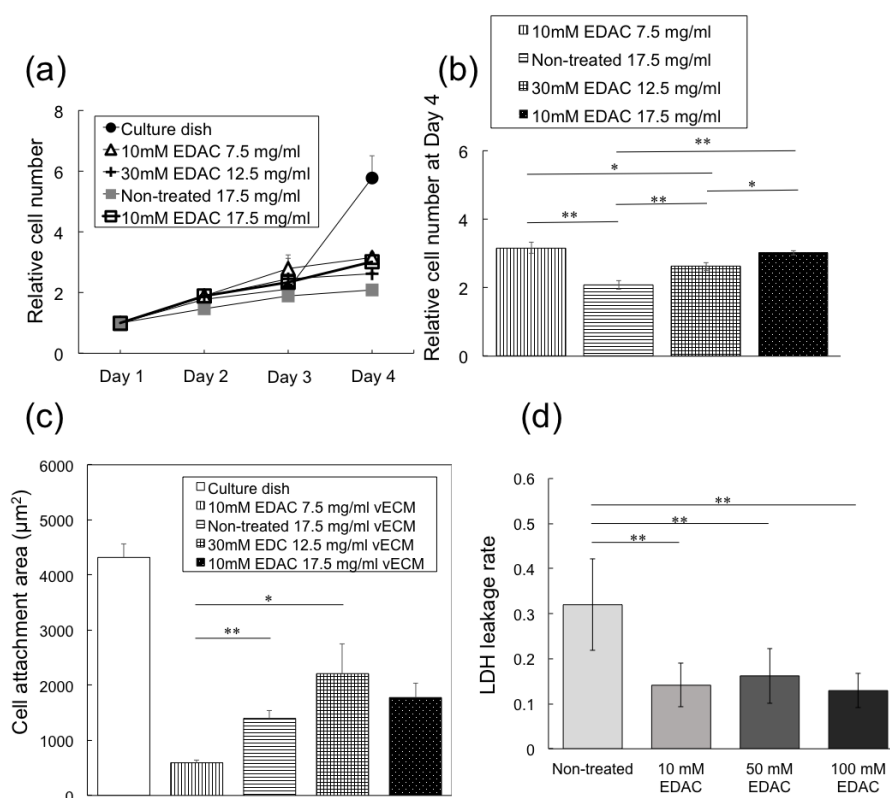


**Figure 10.** (a) Relative cell number of rat embryonic fibroblasts (REFs) on the vECM gels and in the culture dish over 4 days (Mean  $\pm$  SD.  $n = 3$ ). (b) Relative cell number on the 4<sup>th</sup> day with analysis of significance (Mean  $\pm$  SD.  $n = 3$ , \*:  $p < 0.05$ , \*\*:  $p < 0.01$ ). (c) Single cell attachment area on the vECM gels and in the culture dish on the 1<sup>st</sup> day. (Mean  $\pm$  SD.  $n = 30$  cells, \*:  $p < 0.05$ , \*\*:  $p < 0.01$ ). (d) LDH leakage rate of EDAC-treated gels with respect to non-treated gels ( $n = 6$ ). Smaller leakage rate for EDAC-treated gels than non-treated gels shows that EDAC treatment is not harmful and may enhance the cellular compatibility.

Finally, we examined the beat rate of RECs on two EDAC-treated vECM gels. Figure 11 shows the change in the beat rate on 10 mM EDAC-7.5 mg/mL gel and 50 mM EDAC-12.5 mg/mL gel during the 4-day culture. The beat rate of RECs cultured on the 50 mM EDAC-12.5 mg/mL gel was about three times higher than that on the 10 mM EDAC-7.5 mg/mL gel on the first day. However, the beating of RECs on the 50 mM EDAC-12.5 mg/mL gel could not be maintained. By contrast, beating on the 10 mM EDAC-7.5 mg/mL gel, although at a slower rate, was maintained during the 4-day culture.

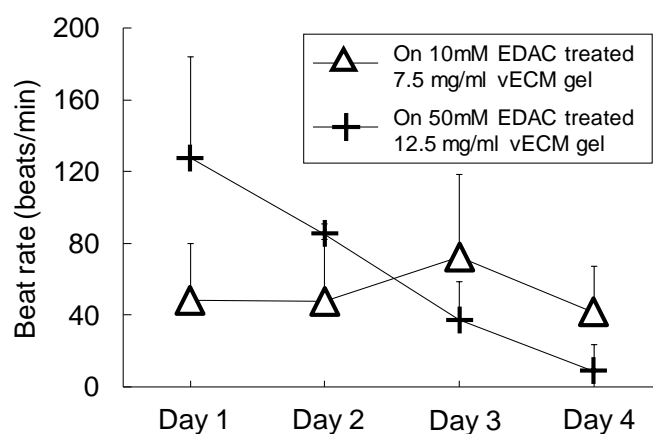


**Figure 11.** Beat rates of the RECs on the EDAC-treated vECM gels over 4 days (Mean + SD.  $n = 4$ ). The faster beating of RECs on the 50 mM EDAC-12.5 mg/mL gel could not be maintained during the culture.

#### 4. Discussion

Although applications of hydrogels made from cardiac ECM and the modulation of mechanical properties of those gels have been reported [17,30–33], this study is distinct in that it is the first to modulate the mechanical properties of hydrogels made from vECM using EDAC crosslinker. In addition, the nonlinear viscoelasticity of the gels was characterized quantitatively using a nonlinear Kelvin-type model newly proposed by our group.

Hydrogels made from ECM solutions are fragile and labile. Increasing the ECM concentration in the hydrogels only resulted in a limited improvement [14,17,30–33]. Although blending with synthetic polymers could enhance the mechanical properties to comparable levels to those of the native tissue [15,16], the factors within the ECM that affect differentiation of stem cells might be disrupted because the combination with foreign materials. Moreover, these methods cannot generate sufficiently stable microstructures that can resist the tense interactions between cells and their surrounding substrates. Such tension might result in the collapse of the microstructure in the vicinity of the cultured cells and even result in a considerable contraction of the whole structure [11,12].

Alternatively, treatment with crosslinkers is an effective way to improve the mechanical properties of hydrogels, as well as stabilizing their microstructure. Crosslinking of cardiac ECM gels with glutaraldehyde (GA) caused a 25-fold increase in gel stiffness [17]. Although GA is a commonly used crosslinker, concerns regarding its immune response and cytotoxicity remain when



the crosslinked substances are used as cell-culture substrates [34]. The unique zero-length crosslinking mechanism of EDAC was appealing for this study. The mechanical properties of collagen gels [35,36], collagen-hyaluronic acid scaffolds [37], and amniotic membranes [38] were improved by treatment with EDAC. In this study, we showed that EDAC crosslinking improved the mechanical properties of the vECM gels, making them comparable to those of the DV tissue. The increase in nonlinearity (Figure 7d) with increasing EDAC and vECM concentrations was consistent with the results of other studies [39,40].

Viscoelasticity of ECM hydrogels made from heart [6,13,15–17,30–33], skeletal muscle [41], urinary bladder [14,42,43], liver [44], and lung [45] has been investigated by complex-modulus measurements. However, complex modulus cannot reflect the nonlinearity of materials. The novelty of this study is that we characterized the nonlinearity and viscoelasticity of the vECM gels using a nonlinear Kelvin model. The compression-relaxation plots (Figures 6a–6c) show clearly that the nonlinear toe region at the beginning of the deformation, and the exponential decay process with one coefficient, can be reproduced by this model. Using this model, we were able to quantify the nonlinearity by the parameter  $\alpha$ , to distinguish the equilibrium elasticity from the instantaneous mechanical response, and to regress the equilibrium elastic modulus  $E$  against the vECM and EDAC concentrations (Eq 7). The effect of EDAC treatment on the stress relaxation coefficient was quite complicated (Figure 7c). The instantaneous mechanical response involved the role of equilibrium elasticity and dissipated elasticity; therefore, we could not find a proper expression for the relation of instantaneous elastic modulus with vECM and EDAC concentrations. However, equilibrium elasticity showed a regular, monotonic dependence on vECM and EDAC concentrations, and could be expressed according to Eq 7. These findings are critically important for tailoring the mechanical properties of vECM gels to make them suitable for cardiomyocyte differentiation.

EDAC-treated scaffolds are reportedly compatible with cell culture [35–37]. This study showed that rat embryonic fibroblasts and cardiomyocytes were cultured fairly well on vECM gels treated with EDAC, which further confirmed the cellular compatibility of the EDAC-treated substrates. The relative cell number of REFs on the vECM gels treated with EDAC was consistently higher than that of REFs on non-treated vECM gels. This result suggested that the unstable structure of non-crosslinked gels might decrease cell division [46].

In this study we mainly aim to develop a 2D substrate for promoting cardiomyocyte performance. The current approach of EDAC treatment to bulky vECM gels is not suitable for 3D scaffold as cells are embedded within. The limitation may be overcome by making thin EDAC-treated gel sheets, culturing cells on these sheets, and stacking them to create a 3D structure. This approach for 3D construction should be confirmed in the future study.

Recently, studies have revealed that the mechanical properties of cell-culture scaffolds or substrates, including viscoelasticity, are critical physical cues for processes related to cellular fate, including the differentiation of stem cells [8,9]. Although the aim of this study was to create pure and stable vECM gels with mechanical properties similar to those of native ventricular ECM, and to examine the cellular compatibility of these gels, the results of the REF and REC cultures still provided brief glimpse into the effects of the mechanical properties of the gels on cellular behavior.

In the REF culture, without considering the non-crosslinked 17.5 mg/mL gels, which had an unstable microstructure, we found that the REFs proliferated rapidly on the gels either with a low

equilibrium elastic modulus (10 mM EDAC-7.5 mg/mL gels;  $E = 17.1 \pm 8.5$  Pa) or with a high modulus (10 mM EDAC-17.5 mg/mL gels;  $E = 246.6 \pm 147.2$  Pa). Normal NIH 3T3 cells tend to proliferate rapidly on stiff substrates [47], which could explain the case of 10 mM EDAC-17.5 mg/mL gels. Why did the REFs grow rapidly on the soft 10 mM EDAC-7.5 mg/mL gels? We hypothesized that the value of the stress relaxation coefficient of the 10 mM EDAC-7.5 mg/mL gels ( $43.4 \pm 32.5$  s) being similar to that of the DV tissue ( $31.4 \pm 9.5$  s) might be responsible for this phenomenon. The change in the cell attachment area might be related to cell proliferation—cells dividing rapidly had small attachment areas (Figures 10a–10c).

For the RECs, although it has been reported that embryonic cardiomyocytes beat best on collagen-coated polyacrylamide gels with heart-like elasticity [48], the influence of viscoelasticity on the behavior of cardiomyocytes has not been investigated. The beat rate profile obtained in this study implied that stiff substrates (50 mM EDAC-12.5 mg/mL gels;  $E = 61.8 \pm 29.7$  Pa) could coordinate the beating of heart cells at a frequency close to that *in vivo*; however, mismatches in the stress relaxation coefficient ( $\lambda = 15.5 \pm 8.4$  s for 50 mM EDAC-12.5 mg/mL gels;  $\lambda = 31.4 \pm 9.5$  s for DV-tissue) eventually resulted in the attenuation of REC beating. However, the abovementioned hypothesis should be further tested using better-tailored gel mechanical properties, which can be achieved based on the outcomes of this study.

## 5. Conclusions

In this study, we developed an easy and rapid protocol to fabricate hydrogels from vECM. The gels were composed of pure vECM and possessed a stable microstructure as a result of crosslinking by using EDAC. Moreover, the crosslinking modulated the mechanical properties of these gels, making their properties closer to those of the decellularized tissue. Using the nonlinear Kelvin model, we could characterize the nonlinearity and viscoelasticity of the gels quantitatively. Furthermore, an empirical relationship between the equilibrium elastic modulus of the gels and the vECM and EDAC concentrations was derived, which is important for tailoring the mechanical properties of the gels. The culture of REFs and RECs on these gels demonstrated the cellular compatibility of the vECM gels crosslinked by EDAC. It also promoted further detailed investigations on the effects of mechanical properties of the vECM gels on the behavior of the cultured cells, with the ultimate aim of using these gels to coax stem cells to differentiate into ventricular cardiomyocytes.

## Acknowledgements

The authors thank Dr. Reiko Nakagawa at RIKEN Kobe Proteomics Facility for the protein identification through mass spectrometry and thank Applied Medical Research Inc. Japan for the histological staining. K.F. are funded by Grant-in-Aid for JSPS Research Fellow from the Japan Society for the Promotion of Science (JSPS) (15J07298) and Z.F., T.K., T.N., and M.U. are funded by Grant-in-Aid for Scientific Research (C) from the Japan Society for the Promotion of Science (JSPS) (17K01352). This work was also partly supported by the Cooperative Research Project Program of Joint Usage/Research Center at the Institute of Development, Aging and Cancer, Tohoku University.

## Conflict of interest

The authors declare that there is no conflict of interest regarding the publication of this manuscript.

## References

1. Vunjak-Novakovic G, Tandon N, Godier A, et al. (2009) Challenges in cardiac tissue engineering. *Tissue Eng Part B* 16: 169–187.
2. Leone M, Magadum A, Engel FB (2015) Cardiomyocyte proliferation in cardiac development and regeneration: a guide to methodologies and interpretations. *Am J Physiol-Heart C* 309: H1237–H1250.
3. Mummery CL, Zhang J, Ng ES, et al. (2012) Differentiation of human embryonic stem cells and induced pluripotent stem cells to cardiomyocytes: a method overview. *Circ Res* 111: 344–358.
4. Schwach V, Passier R (2016) Generation and purification of human stem cell-derived cardiomyocytes. *Differentiation* 91: 126–138.
5. Kempf H, Andree B, Zweigerdt R (2016) Large-scale production of human pluripotent stem cell derived cardiomyocytes. *Adv Drug Deliver Rev* 96: 18–30.
6. Duan Y, Liu Z, O'Neill J, et al. (2011) Hybrid gel composed of native heart matrix and collagen induces cardiac differentiation of human embryonic stem cells without supplemental growth factors. *J Cardiovasc Transl* 4: 605–615.
7. Higuchi S, Lin Q, Wang J, et al. (2013) Heart extracellular matrix supports cardiomyocyte differentiation of mouse embryonic stem cells. *J Biosci Bioeng* 115: 320–325.
8. Engler AJ, Sen S, Sweeney HL, et al. (2006) Matrix elasticity directs stem cell lineage specification. *Cell* 126: 677–689.
9. Chaudhuri O, Gu L, Darnell M, et al. (2015) Substrate stress relaxation regulates cell spreading. *Nat Commun* 6: 6364.
10. Brandl F, Sommer F, Goepferich A (2007) Rational design of hydrogels for tissue engineering: impact of physical factors on cell behavior. *Biomaterials* 28: 134–146.
11. Feng Z, Wagatsuma Y, Kikuchi M, et al. (2014) The mechanisms of fibroblast-mediated compaction of collagen gels and the mechanical niche around individual fibroblasts. *Biomaterials* 35: 8078–8091.
12. Feng Z, Ishiguro Y, Fujita K, et al. (2015) A fibril-based structural constitutive theory reveals the dominant role of network characteristics on the mechanical behavior of fibroblast-compacted collagen gels. *Biomaterials* 67: 365–381.
13. Johnson TD, Lin SY, Christman KL (2011) Tailoring material properties of a nanofibrous extracellular matrix derived hydrogel. *Nanotechnology* 22: 494015.
14. Freytes DO, Martin J, Velankar SS, et al. (2008) Preparation and rheological characterization of a gel form of the porcine urinary bladder matrix. *Biomaterials* 29: 1630–1637.
15. Williams C, Budina E, Stoppel WL, et al. (2015) Cardiac Extracellular Matrix-Fibrin Hybrid Scaffolds with Tunable Properties for Cardiovascular Tissue Engineering. *Acta Biomater* 14: 84–95.

16. Grover GN, Rao N, Christman KL (2014) Myocardial Matrix-Polyethylene Glycol Hybrid Hydrogels for Tissue Engineering. *Nanotechnology* 25: 014011.
17. Singelyn JM, Christman KL (2011) Modulation of material properties of a decellularized myocardial matrix scaffold. *Macromol Biosci* 11: 731–738.
18. Everaerts F, Torrianni M, Hendriks M, et al. (2008) Biomechanical properties of carbodiimide crosslinked collagen: Influence of the formation of ester crosslinks. *J Biomed Mater Res A* 85: 547–555.
19. Fujita K, Tuchida Y, Seki H, et al. (2015) Characterizing and modulating the mechanical properties of hydrogels from ventricular extracellular matrix. *2015 10th Asian Control Conference (ASCC)* 1–5.
20. Kikuchi M, Feng Z, Kosawada T, et al. (2016) Stress relaxation and stress-strain characteristics of porcine amniotic membrane. *Bio-med Mater Eng* 27: 603–611.
21. Johnson TD, DeQuach JA, Gaetani R, et al. (2014) Human versus porcine tissue sourcing for an injectable myocardial matrix hydrogel. *Biomater Sci* 2: 735–744.
22. Ishihama Y, Oda Y, Tabata T, et al. (2005) Exponentially Modified Protein Abundance Index (emPAI) for Estimation of Absolute Protein Amount in Proteomics by the Number of Sequenced Peptides per Protein. *Mol Cell Proteomics* 4: 1265–1272.
23. Fung YC (1993) *Biomechanics: Mechanical properties of living tissues*, 2 Eds, Springer.
24. Fancey KS (2005) A mechanical model for creep, recovery and stress relaxation in polymeric materials. *J Mater Sci* 40: 4827–4831.
25. Feng Z, Matsumoto T, Nakamura T, et al. (2003) Measurements of the mechanical properties of contracted collagen gels populated with rat fibroblasts or cardiomyocytes. *J Artif Organs* 6: 192–196.
26. Ott HC, Matthiesen TS, Goh SK, et al. (2008) Perfusion-decellularized matrix: using nature's platform to engineer a bioartificial heart. *Nat Med* 14: 213–221.
27. Eiselt P, Lee KY, Mooney DJ (1999) Rigidity of Two-Component Hydrogels Prepared from Alginate and Poly(ethylene glycol)-Diamines. *Macromolecules* 32: 5561–5566.
28. Lee KY, Rowley JA, Eiselt P, et al. (2000) Controlling Mechanical and Swelling Properties of Alginate Hydrogels Independently by Cross-Linker Type and Cross-Linking Density. *Macromolecules* 33: 4291–4294.
29. Wang Y, Wang G, Luo X, et al. (2012) Substrate stiffness regulated the proliferation, migration, and differentiation of epidermal cells. *Burns* 38: 414–420.
30. Ungerleider JL, Johnson TD, Rao N, et al. (2015) Fabrication and Characterization of Injectable Hydrogels Derived from Decellularized Skeletal and Cardiac Muscle. *Methods* 84: 53–59.
31. Johnson TD, Dequach JA, Gaetani R, et al. (2014) Human versus porcine tissue sourcing for an injectable myocardial matrix hydrogel. *Biomater Sci* 2: 735–744.
32. Seif-Naraghi SB, Horn D, Schup-Magoffin PA, et al. (2011) Patient-to-patient variability in autologous pericardial matrix scaffolds for cardiac repair. *J Cardiovasc Transl* 4: 545–556.
33. Seif-Naraghi SB, Horn D, Schup-Magoffin PJ, et al. (2012) Injectable extracellular matrix derived hydrogel provides a platform for enhanced retention and delivery of a heparin-binding growth factor. *Acta Biomater* 8: 3695–3703.

34. Huang-Lee LL, Cheung DT, Nimni ME (1990) Biochemical changes and cytotoxicity associated with the degradation of polymeric glutaraldehyde derived crosslinks. *J Biomed Mater Res A* 24: 1185–1201.
35. Cornwell KG, Lei P, Andreadis ST, et al. (2007) Crosslinking of discrete self-assembled collagen threads: Effects on mechanical strength and cell-matrix interactions. *J Biomed Mater Res A* 80: 362–371.
36. Yunoki S, Mori K, Suzuki T, et al. (2007) Novel elastic material from collagen for tissue engineering. *J Mater Sci-Mater M* 18: 1369–1375.
37. Park SN, Park JC, Kim HO, et al. (2002) Characterization of porous collagen/hyaluronic acid scaffold modified by 1-ethyl-3-(3-dimethylaminopropyl) carbodiimide cross-linking. *Biomaterials* 23: 1205–1212.
38. Ma DH, Lai JY, Cheng HY, et al. (2010) Carbodiimide cross-linked amniotic membranes for cultivation of limbal epithelial cells. *Biomaterials* 31: 6647–6658.
39. Piao Y, Chen B (2017) Synthesis and mechanical properties of double cross-linked gelatin-graphene oxide hydrogels. *Int J Biol Macromol* 101: 791–798.
40. Tanpichaia S, Oksmana K (2016) Cross-linked nanocomposite hydrogels based on cellulose nanocrystals and PVA: Mechanical properties and creep recovery. *Compos Part A-Appl S* 88: 226–233.
41. DeQuach J, Lin J, Cam C, et al. (2013) Injectable skeletal muscle matrix hydrogel promotes neovascularization and muscle cell infiltration in a hindlimb ischemia model. *Eur Cells Mater* 23: 400–412.
42. Massensini AR, Ghuman H, Saldin LT, et al. (2015) Concentration-dependent rheological properties of ECM hydrogel for intracerebral delivery to a stroke cavity. *Acta Biomater* 27: 116–130.
43. Wolf MT, Daly KA, Brennan-Pierce EP, et al. (2012) A hydrogel derived from decellularized dermal extracellular matrix. *Biomaterials* 33: 7028–7038.
44. Lee JS, Shin J, Park HM, et al. (2014) Liver extracellular matrix providing dual functions of two-dimensional substrate coating and three-dimensional injectable hydrogel platform for liver tissue engineering. *Biomacromolecules* 15: 206–218.
45. Pouliot RA, Link PA, Mikhael NS, et al. (2016) Development and characterization of a naturally derived lung extracellular matrix hydrogel. *J Biomed Mater Res A* 104: 1922–1935.
46. Ma L, Gao C, Mao Z, et al. (2004) Biodegradability and cell-mediated contraction of porous collagen scaffolds: the effect of lysine as a novel crosslinking bridge. *J Biomed Mater Res A* 71: 334–342.
47. Wang HB, Dembo M, Wang YL (2000) Substrate flexibility regulate growth and apoptosis of normal but not transformed cells. *Am J Physiol-Cell Ph* 279: C1345–C1350.
48. Engler AJ, Carag-Kriegr C, Johnson CP, et al. (2008) Embryonic cardiomyocytes beat best on a matrix with heart-like elasticity: scar-like rigidity inhibits beating. *J Cell Sci* 121: 3794–3802.

